

Evidence for Long-Range Correlations within Arrays of Spontaneously Created Magnetic Vortices in a Nb Thin-Film Superconductor

Daniel Golubchik,* Emil Polturak, and Gad Koren

Department of Physics, Technion-Israel Institute of Technology, Haifa 32000, Israel

(Received 25 November 2009; published 17 June 2010)

We have imaged spontaneously created arrays of vortices (magnetic flux quanta), generated in a superconducting film quenched through its transition temperature at rates around 10^9 K/s. The spontaneous appearance of vortices is predicted by the Kibble-Zurek and by the Hindmarsh-Rajantie models of phase transitions under nonequilibrium conditions. Differentiating between these models requires a measurement of the internal correlations within the emerging vortex array. In addition to short-range correlations predicted by Kibble and Zurek, we found unexpected long-range correlations which are not described by any of the existing models.

DOI: 10.1103/PhysRevLett.104.247002

PACS numbers: 74.78.-w, 74.25.Ha, 85.70.Sq, 98.80.-k

Any physical system undergoing a phase transition within a finite time interval is necessarily driven out of equilibrium. One model that describes the dynamics of such phase transitions is the Kibble-Zurek scenario. The model was first suggested by Kibble [1,2] for cosmological phase transitions which occurred in the early Universe. Kibble proposed that fast cooldown of the Universe, through a critical temperature T_c , leads to formation of initially isolated domains of a new ordered phase. The typical size of a domain, ξ , inside which the emerging order is coherent, is a product of the speed of light and the time needed to complete the phase transition. Consequently, different domains are uncorrelated due to causality. As these disjoint domains coalesce, the mismatch of the order parameter between different regions leads to the appearance of topological defects. The domain size determines both the typical distance and the correlation length between topological defects. Zurek [3] proposed terrestrial tests of this model by examining analogous situations in condensed-matter systems with the same symmetry of the order parameter. The analogous “speed of light” in condensed-matter systems is the velocity of propagation of the order parameter. Since then, some aspects of the Kibble-Zurek (KZ) model have been tested in a variety of physical systems, including liquid helium [4,5], liquid crystals [6], superconductors [7], Josephson junctions [8,9], and superconducting loops [10,11]. Thus, the Kibble-Zurek model is a universal theory of defect formation, whose applications range from phase transitions in grand unified theories to phase transitions observed in different condensed-matter systems. An alternative mechanism of spontaneous vortex formation in superconductors was proposed by Hindmarsh and Rajantie [12,13] (HR). According to this mechanism, thermal fluctuations of the magnetic field freeze inside the superconductor during the transition, creating domains of magnetic flux with the same polarity and characteristic size. In contrast, the KZ model predicts only short-range correla-

tions, with neighboring defects having different topological charge. In a superconductor, where the topological defects are vortices carrying a quantum of magnetic flux, this means that adjacent vortices should have a different polarity. The relative importance of these two mechanisms depends on the Ginzburg-Landau parameter, which is ≈ 1 for Nb, and on critical temperature $T_c \approx 9$ K. The presence of spontaneously generated topological defects was observed in several experiments. Regarding the more sensitive testing of correlations predicted by these models, there is only one experiment on liquid crystals in which an array of topological defects was actually imaged [6]. However, the amount of data was insufficient to detect correlations beyond nearest neighbors. The objective of our experiment is to image spontaneously formed arrays of vortices in a superconductor and measure their correlations.

The experiment requires a technique capable of imaging a relatively large area with a μm resolution. Furthermore, the statistical nature of the problem requires averaging over hundreds of such images. Large areas can be imaged using Hall microscopy [14] or by magneto-optical (MO) imaging [15]. MO imaging has the advantage of being much faster, which is important when many images need to be collected. We have developed a high resolution MO system specifically for this experiment. Our system is described in detail elsewhere [16]. Evaporating the magneto-optical indicator directly on the superconductor’s surface and a cryogenic design suppressing vibrations allowed us to achieve the best spatial resolution ($0.8 \mu\text{m}$) demonstrated so far by this technique. The superconductor sample consists of a 200 nm thick Niobium film deposited on a sapphire substrate. The film was prepared by dc magnetron sputtering, with T_c of 8.9 K. The film is patterned into small squares of $200 \mu\text{m}$ across, to ensure homogeneous illumination by the heating laser pulse and to avoid thermoelectric currents inside the sample. On top of the Nb film, we deposited a 40 nm layer of EuSe, which serves as

the magneto-optic sensor. Because of the huge magneto-optical Kerr effect in EuSe, the polarization plane of linearly polarized light is rotated if the local magnetic field is present. By mapping this rotation at each point of the image, we get an image of the magnetic field directly above the surface of the superconductor. The typical lateral size of a vortex in a Nb film is about 100 nm [17], so the images of individual vortices are diffraction limited. In our setup, observation of individual vortices is possible over a large field of view ($100 \times 100 \mu\text{m}^2$) using a relatively short integration time (10 s), allowing us to acquire many images during an experimental run.

From our previous experiments [7], we know that extremely high cooling rates are essential for spontaneous generation of a measurable amount of vortices. No less important, fast cooling to low temperatures (far below T_c) traps the vortices on pinning centers, preventing annihilation of vortices and antivortices. High cooling rates are achieved in the following way: first, the superconducting film is heated above T_c by a short laser pulse. The film is deposited on a sapphire substrate, which is transparent at the wavelength of the laser. Hence, only the film heats up, while the 1 mm thick substrate remains near the base temperature. At the end of the heating pulse, the heat from the film escapes via ballistic phonons into the cold substrate, which has a thermal mass of ~ 1000 larger than that of the film and acts as a heat sink during the cooldown. The time scale of the heat transfer is much shorter than the length of the laser pulse. Therefore, the cooling rate depends only on the decay time of the laser pulse. We used pulse shaping techniques to change the decay time. In this way, two cooling rates of 4×10^8 and 2×10^9 K/s were achieved. The cooling rates were measured using a GeAu thin-film resistive bolometer. The predicted intervortex spacing is larger than our optical resolution, so that we are able to observe the entire vortex array.

Typical images of spontaneously generated vortex arrays are shown in Fig. 1. During these measurements, the system was carefully shielded from external magnetic fields, and the measured asymmetry between the density of positive and negative vortices was less than 1% (residual field of 10^{-7} T). On average, the two cooling rates we could use, 4×10^8 and 2×10^9 K/s, produced a density of vortices of $6 \times 10^5 \text{ cm}^{-2}$ and $1.3 \times 10^6 \text{ cm}^{-2}$, respectively. The KZ model for 2D predicts a vortex density of $\xi_0^{-2} \sqrt{(dT/dt)\tau_0/T_c}$. Using $\tau_0 = (\pi\hbar)/(16K_B T_c) = 1.7 \times 10^{-13}$ sec [18] and $\xi_0 = 5 \times 10^{-6}$ cm [19], the predicted densities are $7 \times 10^8 \text{ cm}^{-2}$ and $3 \times 10^8 \text{ cm}^{-2}$ for high and low cooling rates, respectively. This is 2 orders of magnitude higher than measured in our experiment. A similar discrepancy was noticed in our earlier work [7]. However, the dependence of the density on the cooling rate is consistent with the KZ model at 2D (proportional to the square root of the cooling rate). Recently, a different dependence was found in small superconducting loops [11].

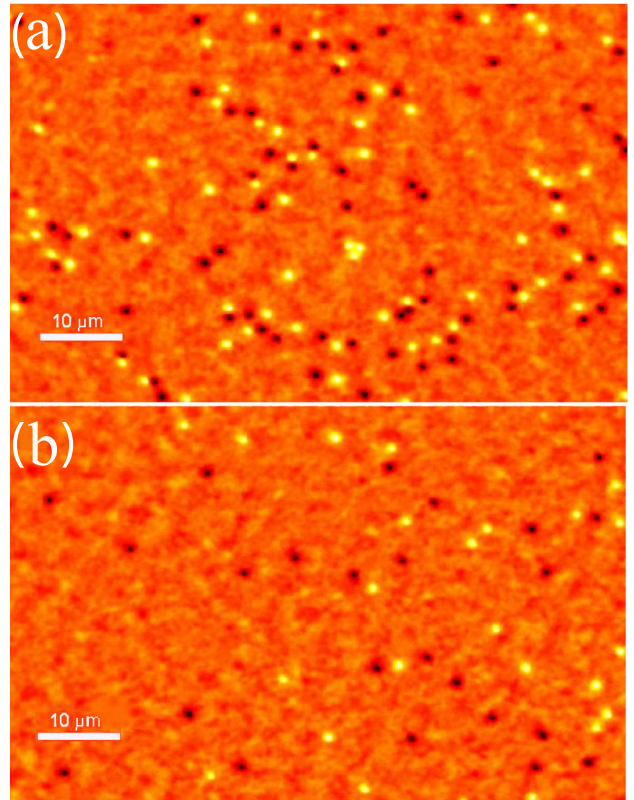


FIG. 1 (color online). Typical images of spontaneously created vortices in a superconductor cooled at (a) 2×10^9 K/s and (b) 4×10^8 K/s. The intensity is proportional to the local magnetic field. Bright and dark spots represent vortices with opposite polarity.

One reason for the low density could be mutual annihilation of nearby vortices having opposite polarities. The attractive force between such vortices increases at short distances. Vortices are prevented from annihilating by pinning forces, which do not depend on the distance. Therefore, a critical distance between vortices with opposite polarity exists, below which pairs of vortices will overcome the pinning force, merge, and annihilate. We attempted to determine this distance by repeating the experiment under external magnetic fields (Fig. 2). The idea is to progressively decrease the distance between vortices of opposite sign. When this distance becomes less than critical, all vortices having an opposite polarity should annihilate. We found that this distance is about $1 \mu\text{m}$. However, the nucleation process can be affected by fields [20] of the order of H_{c1} . In our experiment, the freeze-out temperature $\hat{\epsilon} = 2 \times 10^{-4}$ [3]. Using published data [19] we estimate $H_{c1}(\hat{\epsilon}) \approx 0.1$ mT. The largest field we use is 0.8 mT so the nucleation rate can be biased, and no vortices having polarity opposite to the external field would be created. Consequently, the length which we found is only an upper limit of the critical distance. In any case, in our measurements at zero field (Fig. 1), the typical nearest neighbor separation is $3 \mu\text{m}$, much larger than the critical

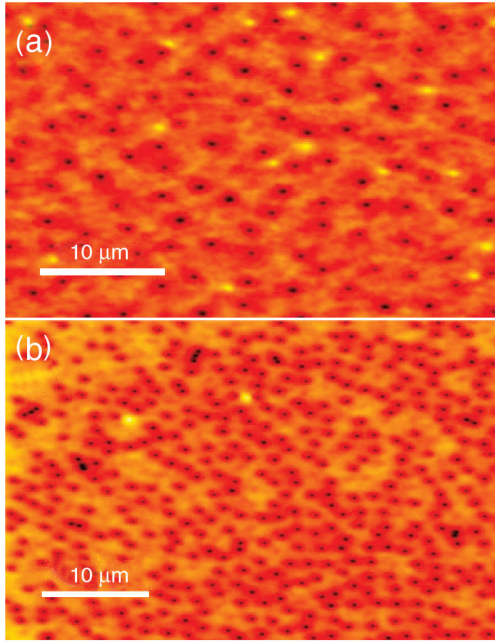


FIG. 2 (color online). Images of magnetic flux in the superconducting film cooled in the presence of an external magnetic field. The external field in (a) is 0.2 mT and in (b) is 4 times larger, 0.8 mT. The cooling rate is 10^9 K/s in both panels. The majority of the vortices (dark spots) are associated with the external magnetic field. Bright spots are vortices with polarity opposite to the field. At higher external fields the number of vortices with opposite sign is reduced.

distance for annihilation. We conclude that at zero field, annihilation does not significantly affect the observed vortex arrays.

We used images like Fig. 1 to determine the correlations between the vortices. In order to increase the statistical ensemble, the correlation function was averaged over 320 such images, with 70 000 vortices in total. We first show the density-density correlation function, irrespective of the vortex polarity. This function is defined as $D(r - r') = \langle \rho(r)\rho(r') \rangle$, where $\rho(r)$ is the local vortex density. The value of $\rho(r)$ is taken to be 1 at the location of a vortex regardless of its polarity, and 0 elsewhere. The natural length scale for correlation is the domain size $\hat{\xi}$, but this parameter is not measured directly. Instead, we scale the distance by the mean vortex separation, $r_{av} = \langle \rho \rangle^{-1/2}$, as proposed by [6]. r_{av} is related to $\hat{\xi}$ by $r_{av} = \frac{\hat{\xi}}{\sqrt{p}}$, where p is the average number of vortices per domain. For our high cooling rate of 2×10^9 K/s, r_{av} is $8.2 \mu\text{m}$. According to the KZ model, if a topological defect is created at some vertex between different domains, the probability to find another defect at the nearest neighbor vertex is higher by 33% than in any other vertex. Consequently, $D(r)$ should show a peak at the characteristic nearest neighbor distance. The correlation function calculated from our data is presented in Fig. 3. There is indeed a peak at $r \approx 0.25r_{av}$,

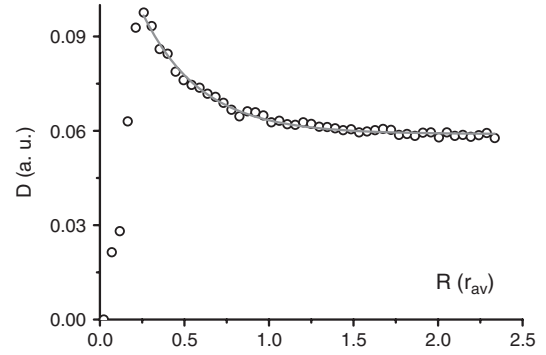


FIG. 3. Density-density correlation function $D(r)$. The cooling rate is 2×10^9 K/s. Distances are in units of $r_{av} = 8.2 \mu\text{m}$. The solid line is a fit to $G(r) \propto r^2 \exp(-r^2/\hat{\xi}^2)$ [21]. The statistical error bars are smaller than the point size.

strong evidence for the short-range correlations predicted by the KZ model. At larger distances, the decay of the peak can be fitted to an exponential dependence, with a decay length of $0.35r_{av}$. According to the KZ model this length is approximately $\hat{\xi}$. From our data, we find that the density of vortices at around the nearest neighbor distance is indeed about 1/3 higher than the mean density.

Next we calculate the correlation function taking into account the polarity of each vortex. The vortex-vortex correlation function is defined as $G(r - r') = \langle n(r)n(r') \rangle$, with $n(r) = 1$ at the location of a positive vortex, -1 at the location of a negative vortex, and 0 elsewhere. The KZ model predicts that nearest neighbor vortices should have opposite polarities. This should manifest itself as a negative peak in $G(r)$. The correlation function was calculated in [21,22]. In both calculations the correlations decay exponentially. In contrast to that, the HR model predicts that neighboring vortices should have the same polarity, and so the peak in the correlation function should be positive. In the KZ model, $\hat{\xi}$ is the only length scale, and both the decay length of the correlations and the characteristic distance between vortices should be $\sim \hat{\xi}$.

Figure 4 shows the vortex-vortex correlation function. The correlation function was multiplied by r to emphasize long-range behavior. The nearest neighbor peak is negative, which indicates that the KZ scenario is the dominant mechanism of vortex formation. The solid line is a fit to the theory of [21] with $\hat{\xi} = 0.35r_{av}$, the same length as in Fig. 3. At distances beyond the peak of Fig. 4 the theoretical correlation function decays to zero, while the experimental correlations do not. Surprisingly, the data show an oscillatory behavior which decays as $\propto r^{-\alpha}$, with $\alpha = 1 \pm 0.5$. This oscillatory behavior is well outside the error margins. No oscillations were measured in the density-density correlation function $D(r)$ (Fig. 3). Hence the oscillations in Fig. 4 represent long-range correlations in the polarity of vortices rather than in their density. We found that the wavelength of these oscillations decreases weakly

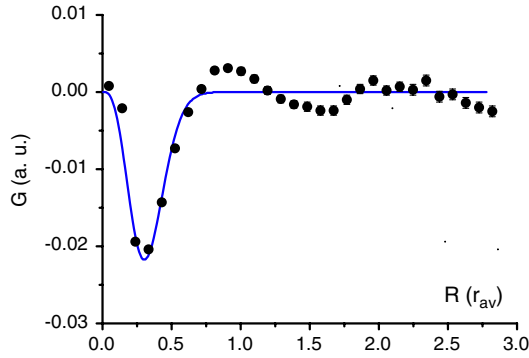


FIG. 4 (color online). First moment of the vortex-vortex correlation function $G(r)$. The negative peak at short distances reflects vortex-antivortex correlations predicted by the KZ model. The solid line is a fit to the theory of [21]. The statistical error bars are smaller than the point size.

with an increasing cooling rate, as well as with the applied magnetic field. One possibility is that these long-range correlations result from some local inhomogeneities in the sample. To check this possibility, we repeated the experiments at several different locations on the film. We found that the correlations were independent of the location. Further, local variations in the local properties such as the value of T_c could potentially modulate the density of vortices, which, however, shows no modulation (Fig. 3), but not the polarity of vortices, which is what we see.

Long-range correlations were predicted in the HR model [12,13]. However, these correlations should decay as r^{-4} , instead of r^{-1} , which we observe, and the predicted domain size is on a mm scale, 2 orders of magnitude larger than the few μm which we see.

For completeness, we mention that unbound vortex-antivortex pairs could arise from the Kosterlitz-Thouless (KT) type of transition. *A priori*, we use thick Nb film for which the transition is of BCS type. Nevertheless, we looked for some signature of the KT vortices. In this theory, the density of unbound vortex pairs above T_{KT} increases with temperature. Consequently, the observed vortex density should depend on the temperature from which the system is quenched. A second prediction is that below T_{KT} the number of surviving vortices decreases linearly with time [23]. Cooling to a temperature where pinning sets in preserves these vortices. Their density should therefore increase linearly with the cooling rate. Within our resolution, we found no dependence on the quench temperature, while the number of vortices we see increases as a square root of the cooling rate.

In cosmology, the size of a domain is determined by the speed of light. The analogous speed in superconductors is the propagation velocity of the order parameter [18,24]. Close to T_c , this speed is $v_s = \hat{\xi}/\hat{\tau} \approx 10^3$ m/s. This speed determines the nearest neighbor distance, the only corre-

lation length in the KZ model. However, vortices are also coupled to an electromagnetic field, which propagates with speed c . Such coupling may perhaps be linked with the longer-range correlations, which are currently a puzzle.

We thank S. Lipson and E. Buks for their contribution to this experiment. We thank S. Hoida, L. Iomin, and O. Shtempluk for technical assistance. This work was supported in part by the Israel Science Foundation and by the Minerva and DIP projects. The authors are grateful to A. Auerbach and D. Podolsky for fruitful discussions.

*danielg@tx.technion.ac.il

- [1] T. W. B. Kibble, *J. Phys. A* **9**, 1387 (1976).
- [2] A. C. Davis and T. W. B. Kibble, *Contemp. Phys.* **46**, 313 (2005).
- [3] W. H. Zurek, *Nature (London)* **317**, 505 (1985).
- [4] C. Bauerle, Y. M. Bunkov, C. N. Fisher, H. Godfrin, and G. R. Pickett, *Nature (London)* **382**, 332 (1996).
- [5] V. M. H. Ruutu, V. B. Eltsov, A. J. Gill, T. W. B. Kibble, M. Krusius, Yu. G. Marhlin, B. Plaais, G. E. Volovik, and Wen Xu, *Nature (London)* **382**, 334 (1996).
- [6] R. Rajarshi and A. Srivastava, *Phys. Rev. D* **69**, 103525 (2004).
- [7] A. Maniv, E. Polturak, and G. Koren, *Phys. Rev. Lett.* **91**, 197001 (2003).
- [8] R. Monaco, J. Mygind, and R. J. Rivers, *Phys. Rev. Lett.* **89**, 080603 (2002).
- [9] R. Carmi, E. Polturak, and G. Koren, *Phys. Rev. Lett.* **84**, 4966 (2000).
- [10] J. R. Kirtley, C. C. Tsuei, and F. Tafuri, *Phys. Rev. Lett.* **90**, 257001 (2003).
- [11] R. Monaco, J. Mygind, R. J. Rivers, and V. P. Koshelets, *Phys. Rev. B* **80**, 180501(R) (2009).
- [12] M. Hindmarsh and A. Rajantie, *Phys. Rev. Lett.* **85**, 4660 (2000).
- [13] A. Rajantie, *Phys. Rev. D* **79**, 043515 (2009).
- [14] S. B. Field, S. S. James, J. Barentine, V. Metlushko, G. Crabtree, H. Shtrikman, B. Ilic, and S. R. J. Brueck, *Phys. Rev. Lett.* **88**, 067003 (2002).
- [15] P. E. Goa, H. Hauglin, A. F. Olsen, M. Baziljevich, and T. H. Johansen, *Rev. Sci. Instrum.* **74**, 141 (2003).
- [16] D. Golubchik, G. Koren, E. Polturak, and S. Lipson, *Opt. Express* **17**, 16160 (2009).
- [17] A. Gauzzi, J. Le Cohec, G. Lamura, B. J. Jönsson, V. A. Gasparov, F. R. Ladan, B. Plaais, P. A. Pronst, D. Pavuna, and J. Bok, *Rev. Sci. Instrum.* **71**, 2147 (2000).
- [18] W. H. Zurek, *Phys. Rep.* **276**, 177 (1996).
- [19] R. A. French, *Cryogenics* **8**, 301 (1968).
- [20] G. J. Stephens, L. M. A. Bettencourt, and W. H. Zurek, *Phys. Rev. Lett.* **88**, 137004 (2002).
- [21] F. Liu and G. F. Mazenko, *Phys. Rev. B* **46**, 5963 (1992).
- [22] R. J. Rivers, *J. Low Temp. Phys.* **124**, 41 (2001).
- [23] H. C. Chu and G. A. Williams, *Phys. Rev. Lett.* **86**, 2585 (2001).
- [24] G. E. Volovik, *Physica B (Amsterdam)* **280**, 122 (2000).